

SODIUM TRANSIENTS IN AN ASTROCYTE

K. Lenk¹, A. Tervonen², J. Hyttinen²

¹Institute for Neural Engineering, Graz University of Technology, Austria

²BioMediTech, Faculty of Medicine and Health Technology, Tampere University, Finland

kerstin.lenk@tugraz.at

Abstract— Astrocytes, a type of glial cells in the brain, are actively involved in neuronal information processing and memory formation. An astrocyte participates in neuronal activity by receiving neurotransmitters, e.g., glutamate, from an adjacent pre-synapse. This leads to the propagation of astrocytic intra- and intercellular calcium waves. In this study, we extend the computational model presented by Oschmann et al. (2017) to a finite element model of single astrocytes, including a realistic 2D geometry and inositol 1,4,5-trisphosphate (IP₃) and ion diffusion. Here, we conduct a parameter exploration of the sodium-calcium exchanger (NCX) and sodium-potassium-ATPase (NKA) rate constants. The calcium concentration directly depends on the amplitude of the glutamate stimulus. However, the sodium concentration instead relates only to the sodium-potassium pump activity.

Keywords— Astrocyte, simulation, sodium, calcium, diffusion

Introduction

Astrocytes are a glial cell type that plays a major role in the ion and energy homeostasis of the brain. Astrocytes and neurons are in a ratio of 1:2 in rodents and even 1:1 in humans. A single astrocyte can connect between 270 000 and 2 million neuronal synapses [1]. Thus, astrocytes can functionally modulate neuronal activity and complex mammalian behavior. In a landmark paper [2], mice with transplanted human astrocytes showed improved long-term potentiation and performance in learning tasks, emphasizing the importance of human astrocytes for the unique human cognitive abilities. Experimental findings strongly indicate that astrocytes might be involved in various pathologies such as epilepsy, depression, Alzheimer's, and Huntington's disease [3], [4]. Computational modeling can aid experimental work by forming a theoretical framework to characterize the anatomy and function of neurons and astrocytes [5]. Thus, a well-planned theoretical study can guide experimentalists towards the most relevant experiments, and in this way, save time and resources. In our review paper [5], we summarized astrocyte models from subcellular to network level that have started to emerge.

Oschmann et al. [6] introduced an astrocyte model including two glutamate pathways which both induce calcium (Ca²⁺) elevations (Fig. 1): activation of (1) the metabotropic glutamate receptors (mGluRs) and (2)

the glutamate transporters (mGluT) at the plasma membrane. The mGluR pathway includes the uptake of glutamate from the extracellular space. Subsequently, inositol 1,4,5-trisphosphate (IP₃) followed by a Ca²⁺ release from the endoplasmic reticulum (ER) into the cytosol through IP₃ receptor channels. The increasing Ca²⁺ levels lead to an opening of further IP₃ channels and a Ca²⁺-induced Ca²⁺ release (CICR). The second pathway includes the mGluTs, which transports potassium (K⁺) out and sodium (Na⁺) and glutamate into the cell. Furthermore, the sodium-calcium exchanger (NCX) exchanges Na⁺ and Ca²⁺ ions. The Na⁺-K⁺-ATPase (NKA) transports Na⁺ ions out and K⁺ ions into the cell. Additionally, leak currents for Na⁺ and K⁺ are modeled. The novelty of the model is the combination of those two pathways and their dependence on the surface-to-volume ratio (SVR) and ER amount in the respective cell section. The SVR is large in perisynaptic astrocytic processes that connect to the neurons and small in the soma of the astrocyte. The ER ratio behaves the opposite.

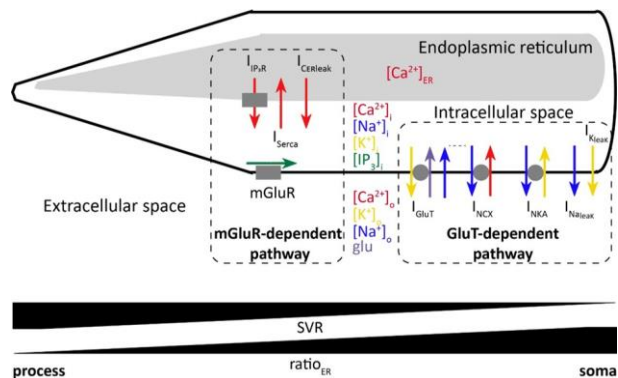


Figure 1: Scheme of the calcium dynamics within an astrocyte, including the mGluR- and the GluT-dependent pathway (adapted from [6]).

In this study, we combined the model by Oschmann et al. with a whole-cell astrocyte morphology [7]. Based on the width of a cell section, we automatically calculated the SVR. Furthermore, we added IP₃ and ion (Ca²⁺, K⁺, and Na⁺) diffusion to the model.

Methods

We used the model and its parameters as described in Oschmann et al. [7] with the following additions: diffusion of IP₃, Ca²⁺, K⁺, and Na⁺ with coefficients 300, 13, 1 960, and 1 330 μm²/s, respectively. Our model was implemented as a finite-

element method with a realistic geometry (Fig. 2 top) in COMSOL Multiphysics version 5.6. The geometry is implemented in 2D as a tridomain model (i.e., ER, cytosol, and extracellular space). The SVR in the geometry required by the model was based on the width of the processes.

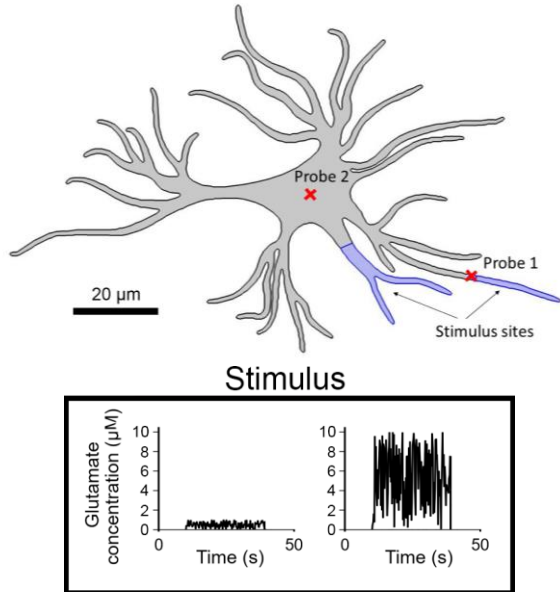


Figure 2: Top: Geometry of a single astrocyte with an indication of the stimulus sides (blue) and the locations of the two measurement probes (red crosses). Bottom: Random (uniform distribution) stimuli from 10 to 40 s with either 0.5 μM or 5 μM mean glutamate concentration.

We conducted a parameter exploration for the maximum pump current of NCX, I_{NCXmax} , with the values 10^{-6} , 10^{-5} , 10^{-4} , 10^{-3} , 0.01, and 0.1 pA/μm², and for the maximal pump activity of NKA, I_{NKAmx} , with the values 10^{-6} , 0.1, 0.5, 1, 1.52, and 5 pA/μm². Similar parameter ranges have also been explored in Oschmann et al. [6]. Furthermore, we applied two different random glutamate stimuli with a mean of around 0.5 and 5 μM (Fig. 2 bottom) to two processes (Fig. 2 top).

For the different I_{NCXmax} and I_{NKAmx} values and the two glutamate input values, we measured the Ca²⁺ and Na⁺ concentrations in one of the stimulated processes (Probe 1) and the soma of the astrocyte (Probe 2). Moreover, we counted the number of Ca²⁺ events (i.e., Ca²⁺ spikes with a full width at half maximum of maximally five seconds). We also determined the maximum values of the Na⁺ concentration during the stimulation time as a function of the pump currents and the glutamate stimulus.

Results

Fig. 3 shows the Ca²⁺ concentrations in Probe 1 and 2 for the two applied glutamate concentrations. The higher stimulus led to more distinct Ca²⁺ spikes.

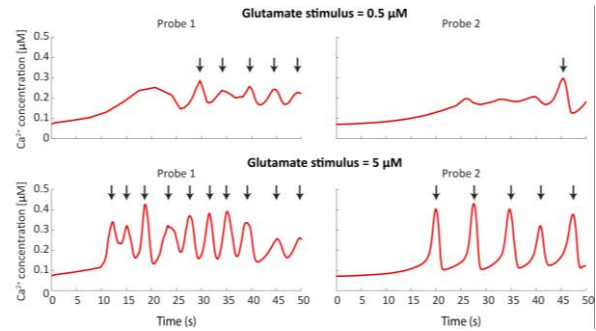


Figure 3: Ca²⁺ concentrations after stimulating the astrocyte with a glutamate concentration of 0.5 or 5 μM and applying $I_{NCXmax} = 0.1$ pA/μm² and $I_{NKAmx} = 1$ pA/μm². Rows: Glutamate stimulus of 0.5 (top) or 5 μM (bottom). Columns: Ca²⁺ concentrations in Probe 1 (left) or 2 (right) during the stimulation time. The arrows indicate the Ca²⁺ peaks. The x-axis depicts the time in seconds.

The maximum number of Ca²⁺ events was yielded with a glutamate stimulus of 5 μM and $I_{NCXmax} = 0.1$ pA/μm² and $I_{NKAmx} = 1$ pA/μm² (Fig. 4). As expected, the number of spikes was higher for a higher glutamate stimulus. For smaller I_{NKAmx} values and higher I_{NCXmax} values, the most number of Ca²⁺ oscillations were detectable.

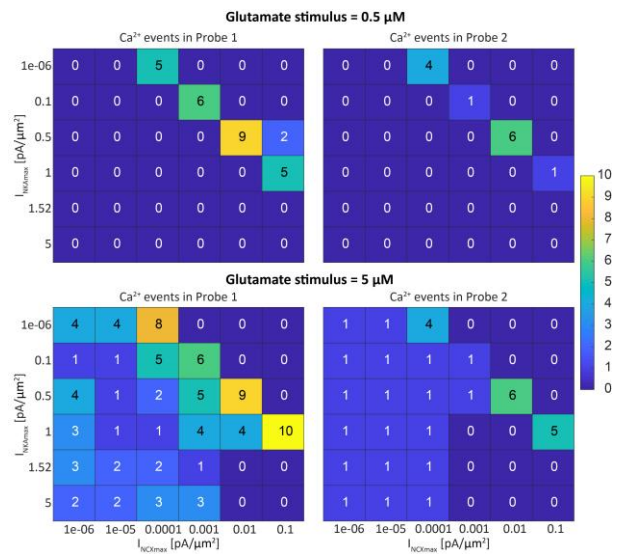


Figure 4: Number of Ca²⁺ events after stimulating the astrocyte with a glutamate concentration of 0.5 or 5 μM and different values for I_{NCXmax} and I_{NKAmx} . Rows: Glutamate stimulus of 0.5 (top) or 5 μM (bottom). Columns: Number of Ca²⁺ events (color bar) in Probe 1 (left) or 2 (right) during the stimulation time.

The maximum Na⁺ concentration was clearly dependent on the values of I_{NKAmx} rather than on the values of I_{NCXmax} and the glutamate concentration (Fig. 5). The lower the values of I_{NKAmx} was the higher the Na⁺ concentration.

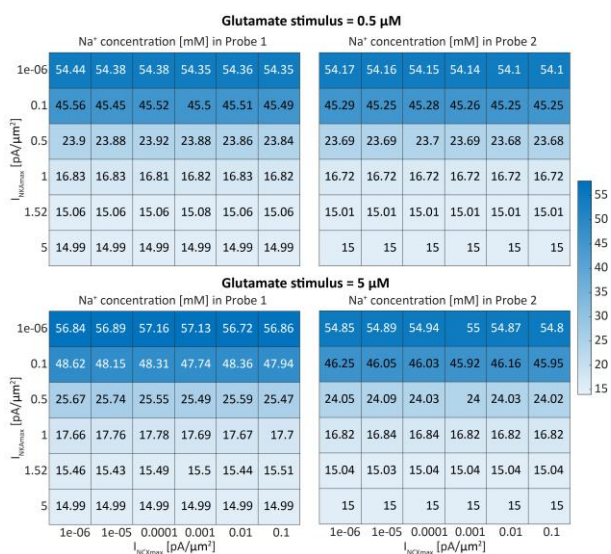


Figure 5: Na⁺ concentrations after stimulating the astrocyte with a glutamate concentration of 0.5 or 5 μM and different values for INCX_{max} and INK_{Amax}. Rows: Glutamate stimulus of 0.5 (top) or 5 μM (bottom). Columns: maximum Na⁺ concentrations (color bar) in Probe 1 (left) or 2 (right) during the stimulation time.

Discussion

Our computational model investigates the intracellular calcium and sodium concentrations in dependence on the glutamate stimulus as well as the sodium-calcium exchanger, NCX, and the sodium-potassium-ATPase, NKA, pump rates. Therefore, we have extended the model by Oschmann et al. [7] by a realistic geometry and IP₃ and ion diffusion.

There is a complex interplay between the calcium and sodium dynamics in the astrocyte. Calcium signals and oscillations may be triggered by activated mGluRs [8], [9] as well as by the NCX in reverse mode [10] and the inhibition of NKA [11]. In a study by Ziemens et al. [12], the authors used the equation of the NCX model as also used in [7]. They found that after glutamate-induced stimulation, the NCX switches from an inward mode to an outward/ reverse mode, which is connected to a calcium influx to the astrocyte. Furthermore, the model suggests that the calcium increase only weakly antagonizes the NCX in the processes but not in the soma.

Our study suggests that the intracellular sodium concentration is mainly driven by the NKA. A blockage of the NKA transporter by ouabain led to an increase of cytosolic sodium concentrations and thus seems to be the primary cause for sodium elevations in the astrocyte [10].

To conclude, our simulations showed that the calcium levels depend on the given glutamate concentrations and a balance of the sodium-calcium exchanger and the sodium-potassium-ATPase pump rates.

The sodium levels rather relate only to the sodium-potassium pump activity.

Acknowledgements

K.L. received funding from the Academy of Finland (decision nos. 314647, 326452).

References

- [1] T. Papouin, J. Dunphy, M. Tolman, J. C. Foley, and P. G. Haydon, "Astrocytic control of synaptic function," *Philos. Trans. R. Soc. B Biol. Sci.*, vol. 372, no. 1715, p. 20160154, 2017, doi: 10.1098/rstb.2016.0154.
- [2] X. Han *et al.*, "Forebrain engraftment by human glial progenitor cells enhances synaptic plasticity and learning in adult mice," *Cell Stem Cell*, vol. 12, no. 3, pp. 342–53, Mar. 2013, doi: 10.1016/j.stem.2012.12.015.
- [3] D. A. Coulter and C. Steinhäuser, "Role of Astrocytes in Epilepsy," *Cold Spring Harb Perspect Med*, vol. 5, p. a022434, 2015, doi: 10.1038/clpt.2011.183.
- [4] A. M. Wójtowicz, A. Dvorzhak, M. Semtner, and R. Grantyn, "Reduced tonic inhibition in striatal output neurons from Huntington mice due to loss of astrocytic GABA release through GAT-3.," *Front. Neural Circuits*, vol. 7, no. November, pp. 1–12, Nov. 2013, doi: 10.3389/fncir.2013.00188.
- [5] F. Oschmann, H. Berry, K. Obermayer, and K. Lenk, "From in silico astrocyte cell models to neuron-astrocyte network models: A review," *Brain Res. Bull.*, vol. 136, pp. 1–9, Jan. 2017, doi: 10.1016/j.brainresbull.2017.01.027.
- [6] F. Oschmann, K. Mergenthaler, E. Jungnickel, and K. Obermayer, "Spatial separation of two different pathways accounting for the generation of calcium signals in astrocytes," *PLoS Comput. Biol.*, vol. 13, no. 2, pp. 1–25, 2017, doi: 10.1371/journal.pcbi.1005377.
- [7] M. U. Khalid, A. Tervonen, I. Korkka, J. Hyttinen, and K. Lenk, "Geometry-based Computational Modeling of Calcium Signaling in an Astrocyte," in *Proc. EMBEC'17 & NBC'17*, 2017, pp. 157–160, doi: 10.1007/978-981-10-5122-7_40.
- [8] A. H. Cornell-Bell, S. M. Finkbeiner, M. S. Cooper, and S. J. Smith, "Glutamate induces calcium waves in cultured astrocytes: Long-range glial signaling," *Science (80-.)*, vol. 247, no. 4941, pp. 470–473, Jan. 1990, doi: 10.1126/science.1967852.
- [9] S. Kirischuk, F. Kirchhoff, V. Matyash, H. Kettenmann, and A. Verkhratsky,

“Glutamate-triggered calcium signalling in mouse Bergmann glial cells in situ: Role of inositol-1,4,5-trisphosphate-mediated intracellular calcium release,”

Neuroscience, vol. 92, no. 3, pp. 1051–1059, Jun. 1999, doi: 10.1016/S0306-4522(99)00067-6.

- [10] R. C. Reyes, A. Verkhratsky, and V. Parpura, “Plasmalemmal Na⁺/Ca²⁺ exchanger modulates Ca²⁺-dependent exocytotic release of glutamate from rat cortical astrocytes,” doi: 10.1042/AN20110059.
- [11] X. L. Liu, A. Miyakawa, A. Aperia, and P. Krieger, “Na,K-ATPase generates calcium oscillations in hippocampal astrocytes,” *Neuroreport*, vol. 18, no. 6, pp. 597–600, Apr. 2007, doi: 10.1097/WNR.0b013e3280b07bc9.
- [12] D. Ziemens, F. Oschmann, N. J. Gerkau, and C. R. Rose, “Heterogeneity of Activity-Induced Sodium Transients between Astrocytes of the Mouse Hippocampus and Neocortex: Mechanisms and Consequences,” *J. Neurosci.*, vol. 39, no. 14, pp. 2620–2634, 2019, doi: 10.1523/jneurosci.2029-18.2019.